Modulation of epsilon-near-zero wavelength and enhancement of third-order optical nonlinearity in ITO/Au multilayer films

Bin Guo (郭 斌), Zhongshuai Zhang (张中帅), Yanyan Huo (霍燕燕), Shuyun Wang (王书运)[*], and Tingyin Ning (宁廷银)[**]

Shandong Provincial Engineering and Technical Center of Light Manipulations & Shandong Provincial Key Laboratory of Optics and Photonic Device, School of Physics and Electronics, Shandong Normal University, Jinan 250358, China

*Corresponding author: wangsy@sdnu.edu.cn
**Corresponding author: ningtingyin@sdnu.edu.cn

We report the modulation of epsilon-near-zero (ENZ) wavelength and enhanced third-order nonlinearity in indium tin oxide (ITO)/Au multilayer films. The samples consisting of five-layer 40 nm ITO films spaced by four-layer ultrathin Au films of different thickness, i.e., ITO(40 nm)/[Au(x)/ITO(40 nm)]$_4$, were prepared by magnetron sputtering at room temperature. The ENZ wavelength in the multilayer films is theoretically calculated and experimentally confirmed. The nonlinear refractive index and nonlinear absorption coefficient of the samples of $x = 0, 2, 3, 4$ nm were determined using the Z-scan method at a wavelength of 1.064 μm. The large nonlinear refractive index $n_2 = 1.12 \times 10^{-13}$ m^2/W and nonlinear absorption coefficient $\beta = -1.78 \times 10^{-7}$ m/W in the sample of $x = 4$ nm are both four times larger than those in the single-layer ITO film. The large optical nonlinearity due to the ENZ enhancement and carrier concentration is discussed. The results indicate that the ITO/Au multilayer films are promising for advanced all-optical devices.

Keywords: third-order nonlinearity; epsilon-near-zero wavelength; multilayer.
DOI: 10.3788/COL202321.013602

1. Introduction

Material that possesses strong and ultrafast nonlinear optical response and is compatible with the complementary metal-oxide semiconductor (CMOS) fabrication technologies is essential for the high-performance integrated on-chip nonlinear optical devices, such as all-optical signal processing, computing, and communicating[1]. Recently, materials of free charges were widely reported to possess the extremely large third-order non-linearity at their epsilon-near-zero (ENZ) frequencies, which show their promise for applications in nonlinear optics[2]. Indium tin oxide (ITO), as one of the typical CMOS-compatible and ENZ materials working at near-infrared, draws more attention since the extremely large effective nonlinear refractive index and nonlinear absorption coefficient measured at angle of incidence 60° were found to be around 43 and 45 times larger than those obtained at the normal incidence[3]. The nonlinear refractive index as large as 3.73 ± 0.56 cm^2/GW was further obtained at the ENZ wavelength in the Au nanoantennas coupled to ITO films[4]. The large nonlinear refractive index $(1.543 \times 10^{-15}$ m^2/W) and nonlinear saturable absorption coefficient $(-6.48 \times 10^{-9}$ m/W) were also recently obtained in ITO/Ag/ITO sandwiches[5].

However, the ENZ wavelength of ITO and other ENZ materials, is governed by the intrinsic material properties and occurs at a special regime[6], which limits their applications for photonic devices working at a broad band. Though the ENZ wavelength of ITO can be modulated by controlling the fabrication parameters[7], it is still working limitedly in the near-infrared wavelength regime, which is determined by the intrinsic properties. The layered metal-dielectric multilayer stacks offer an effective and simple way to tune the effective ENZ wavelength[8]. The effective permittivity of multilayer stacks can be calculated using the formula $\varepsilon_{\text{eff}} = f_a \varepsilon_a + f_b \varepsilon_b$ when the polarization of the electric field is parallel to the plane of the layers, where f_a and f_b refer to the volume fraction of material a and material b with $f_a + f_b = 1$; ε_a and ε_b are the permittivities of layers a and b, respectively[9]. The combination of the noble metals possessing ENZ behavior in the UV region and particular dielectrics of ENZ behavior in the infrared region can extensively modulate the effective ENZ wavelength covering from the UV to infrared region in such composites and further modify the effective optical nonlinearity in a wide band for nonlinear devices. Though the enhanced third-order optical nonlinearity in layered metal-dielectric multilayer stacks with ENZ behavior at visible

wavelength has been reported by Suresh et al.[8], the dielectric materials SiO$_2$ of negligible nonlinear response were used, and only the nonlinearity from Ag is involved. The dominant optical nonlinearity in the dielectric layer in multilayer films of tunable ENZ wavelength is still lacking investigation.

In this Letter, we report the modulation of ENZ wavelengths and third-order nonlinearity in ITO/Au multilayer films. The ENZ wavelength was tuned to be around 0.94 µm and 1.29 µm in the multilayers consisting of five-layer ITO film (each layer thickness 40 nm) and inserted four-layer Au of each layer thickness of 3 and 4 nm, respectively. The large nonlinear refractive index and nonlinear absorption coefficient measured at 1.064 µm were obtained, which are four times larger than those in the pure ITO film. The results show that the ITO/Ag multilayer films are promising candidate materials for all-optical devices working at a desired wavelength.

2. Experimental Details

The theoretical effective permittivity of multilayer stacks based on the reported dielectric constant of ITO[3] and Au[10] is shown in Fig. 1(a). It is clear that the ENZ wavelength of ITO/Au multilayer films can obviously be modulated with the increase of the filling factor of Au f_{Au}. Experimentally, the ITO/Au/ITO (IAI) multilayer films and pure ITO films were prepared on fused silica substrates (20 mm × 20 mm × 0.5 mm) at room temperature using the magnetron sputtering method. The base pressure of the chamber was pumped to be 6.0×10^{-4} Pa, and the substrate was rotated at a uniform speed of 15 revolutions per minute to ensure uniform film thickness during the deposition. During the deposition, the DC power was kept at 120 W and Ar flow as 20 sccm (standard cubic centimeters per minute). The deposition rate is around 1 nm/s. The ITO target was a 10% (mass fraction) SnO$_2$-doped In$_2$O$_3$ disk (purity 99.99%), and an Au target of purity 99.99% was used for the deposition. The multilayer films consist of five-layer 40 nm ITO films and four-layer Au films of different thickness of $x = 2$, 3, and 4 nm inserted between the ITO layers, i.e., ITO(40 nm)/ [Au(x)/ITO(40 nm)]$_4$, denoted as IAI-2, IAI-3, and IAI-4, respectively. The schematic structure of the multilayer film is shown in Fig. 1(b). The pure ITO film of thickness 200 nm was fabricated and denoted as pure ITO. The growth rate of each layer was determined by the quartz crystal oscillator, and the desired thickness of each was controlled by the sputtering time, which was further examined by scanning electron microscopy (SEM).

3. Results and Discussion

The cross section of the IAI-4 multilayer film measured by SEM is shown in Fig. 1(c). The interfaces between ITO and Au are observed, and the thickness of each layer is uniform. The total thickness is measured to be around 221 nm, which is close to the expected thickness of 216 nm controlled by the growth rate and sputtering duration. The surface morphology of the IAI-4 film in
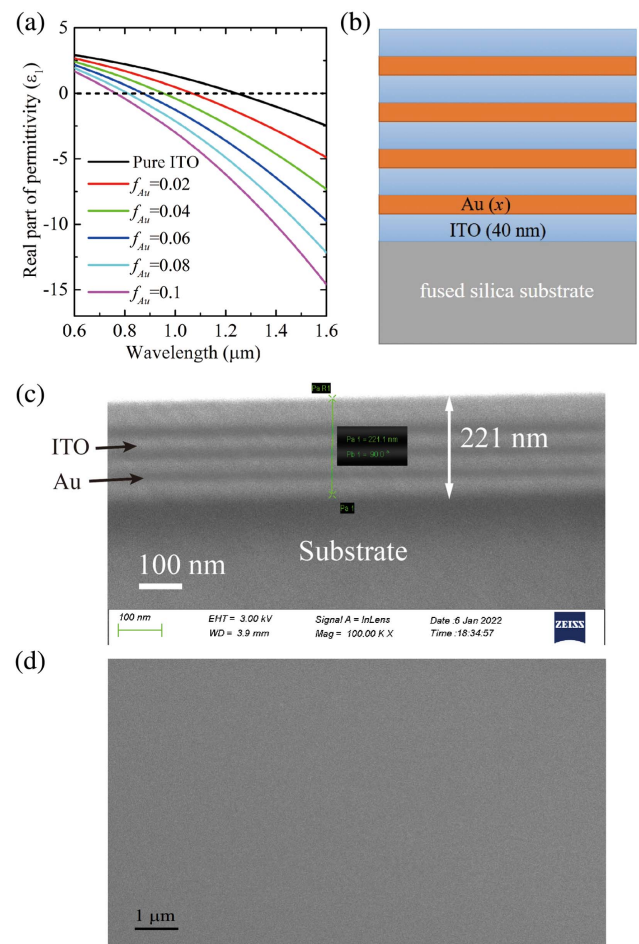

Fig. 1. (a) Theoretical real part of effective permittivity of ITO/Au multilayer stacks. (b) Schematic diagram of an ITO-Au multilayer stack. (c) Cross-sectional image and (d) surface morphology of the IAI-4 multilayer film obtained by SEM.

Fig. 1(d) indicates that the film has a very compact and uniform surface in the large scale. No cracks and large particles were observed on the surface of the film.

The crystallization of the pure ITO and IAI multilayer films was characterized by X-ray diffraction (XRD). The XRD patterns of the pure ITO and IAI-4 films are shown in Fig. 2. The diffraction peaks in the pure ITO film indicate the 200 nm ITO film has a polycrystalline structure. However, there are no obvious peaks from ITO in the IAI-4 multilayer film. This is probably ascribed to the fact that the crystallization of ITO is influenced by the thickness. During the growth, the accumulation of sputtering may help to materialize the crystallization due to the tension, and thus the polycrystalline structure is formed in 200 nm ITO film, but not in 40 nm ITO film. The Au (222) peak is clearly observed in the IAI-4 film. The crystallite size of Au is estimated to be about 5.2 nm, which is close to the nominal thickness of 4 nm, using the Scherrer equation $\langle L \rangle = K\lambda/w \cos\theta$, where $\langle L \rangle$ is the average crystallite size in the direction perpendicular to the reflecting plane, K is a constant at 0.89, λ is the X-ray wavelength, w is the full width at half maximum of the diffraction peak, and θ is the diffraction angle.
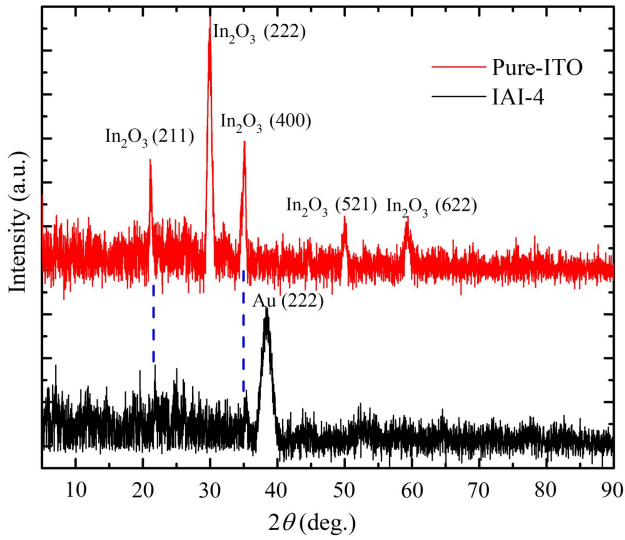
Fig. 2. XRD patterns of the pure ITO film and IAI-4 multilayer film.

The refractive index n and extinction coefficient κ of the films were determined by an ellipsometer in the range of 0.6–1.7 μm. The permittivity ε is obtained from the refractive index n and extinction coefficient κ, which were determined from ellipsometer data by $\varepsilon = (n + i\kappa)^2 = \varepsilon_1 + i\varepsilon_2$. The real ($\varepsilon_1$) and imaginary ($\varepsilon_2$) parts of dielectric permittivity in pure ITO film and the effective permittivity of the multilayer films are shown in Fig. 3. Note that the ENZ wavelength of the pure ITO film would beyond 1.7 μm, which is out of the range of our ellipsometry instrument. It is probably due to the atom derivation and microstructures in the films drawn by the preparation parameters, which was also found in Ref. [7]. When the Au layers are inserted in the ITO/Au multilayer stacks, the permittivity is effectively modulated. When Au layer is 2 nm, the ENZ wavelength is still beyond 1.7 μm. The ENZ wavelength is clearly observed and is around 0.94 μm and 1.29 μm when the Au layer achieves 3 nm and 4 nm, respectively. The results show that the ENZ wavelength is indeed modulated in the multilayer stacks by changing the fill factor of noble metal. The change agrees well
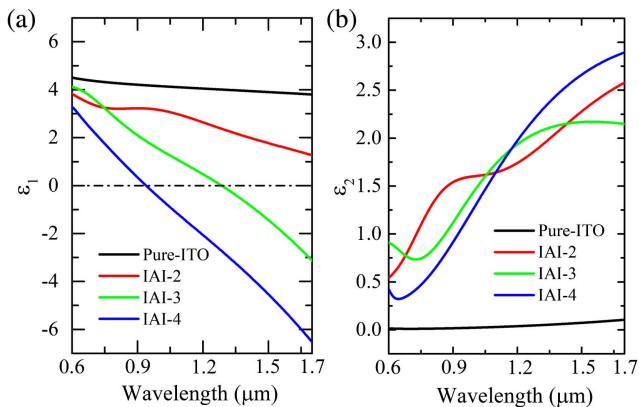
with the theoretical prediction [Fig. 1(a)], i.e., the increase of Au volume fraction will lead to the blueshift of ENZ wavelength. The ENZ wavelength could be further blue-shifted with the increase of the thickness of the Au layer and fall into the visible region. Note that the imaginary part of effective permittivity ε_2 of multilayer films significantly increased compared to the pure ITO film, which is detrimental to the photonic devices. Next, we will see that the large ε_2 does not affect the enhancement of optical nonlinearity, but is still a worthy concerned parameter for the design of photonic devices.

The third-order optical nonlinearity of the samples was investigated using a single-beam Z-scan method[11]. The typical Z-scan experimental setup for measurements is similar to that used in our previous works[12,13]. In brief, a Nd:Y$_3$Al$_5$O$_{12}$ (Nd:YAG) laser with a wavelength of 1.064 μm and pulse duration of 25 ps was used as the light source. The focal length of the lens before the samples was 150 mm, which leads to the radius of the beam waist around 40 μm and the peak intensity around 16 GW/cm^2. The power of the reference beam and the transmitted beam was recorded by the detectors connected to the power meter (PM320E, Thorlabs Inc.), respectively. The linear transmission of the far field S was set to be 0.2. For each sample, the Z-san measurement was conducted at 20 different positions to ensure the homogeneity of the samples. The uncertainty of the determined values of nonlinear absorption and refractive index is around 20%. The representative normalized transmittances, as well as their theoretical fitting curves, of the samples measured under the open-aperture (OA) and closed-aperture (CA) Z-scan method are shown in Fig. 4. The nonlinear optical response of the fused silica substrate is quite weak and negligible under such laser intensity, so the patterns of OA and CA measurements are from the samples. The peak patterns of OA Z-scan curves in the samples indicate that all samples possess saturation absorption. The CA Z-scan curves of the samples all show valley-peak patterns, indicating that the samples have self-focusing effects and positive nonlinear refractive index. The calculated values of β and n_2 are given in Table 1. It is noted that the values in this work are much larger than those reported in the references,

Fig. 3. Experimentally determined permittivity of the pure ITO film and effective permittivity of the multilayer films.
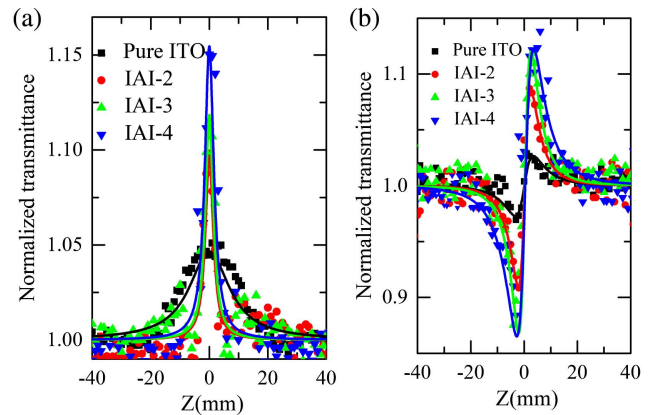

**Fig. 4.** (a) OA and (b) CA Z-scan data with the theoretical fittings for pure ITO film and multilayer films.

Table 1. Saturable Absorption Coefficient β, Nonlinear Refractive Index n_2, and Carrier Concentrations in the Samples.

Sample	β ($\times 10^{-8}$ m/W)	n_2 ($\times 10^{-14}$ m^2/W)	Carrier Concentrations ($\times 10^{21}$ cm^{-3})
Pure ITO	−4.99	2.55	0.13
IAI-2	−11.64	8.01	1.13
IAI-3	−13.89	11.16	4.98
IAI-4	−17.80	11.21	6.86

Fig. 5. Carrier concentration, resistivity, and nonlinear optical response versus the thickness of the Au layer.

which is ascribed to the probably involved thermal nonlinearity due to the employed picosecond-pulsed laser source.

It is obvious that the nonlinear optical response in the multilayer films is efficiently enhanced compared with that in the pure ITO film. The saturable absorption coefficient β and nonlinear refractive index n_2 achieve their maximum values in the IAI-4 film. Compared to the β and n_2 in the pure ITO film, the β and n_2 in the IAI-4 film both increase around four times. The optical nonlinearity of Au film at 1.064 µm is too weak to exhibit the typical OA and CA Z-scan patterns below the laser damage threshold. Given that the nonlinearity of the multilayer films satisfies the nonlinear effective medium theory, i.e., $\chi_{\text{eff}}^{(3)} = f_a\chi_a^{(3)} + f_b\chi_b^{(3)}$, where $\chi_{\text{eff}}^{(3)}, \chi_a^{(3)}$, and $\chi_b^{(3)}$ are the effective third-order nonlinear susceptibilities of the composite material and materials a and b, respectively. If the nonlinearity of Au is neglected, the multilayer films have the effective third-order nonlinear susceptibility $\chi_{\text{eff}}^{(3)} = f_{\text{ITO}}\chi_{\text{ITO}}^{(3)}$. Since $f_{\text{ITO}} < 1$, the ITO/Au multilayer films will give a smaller $\chi^{(3)}$ than that of the pure ITO film. However, the values of n_2 in multilayer films are larger than that in the pure ITO film, especially, the n_2 of IAI-3 and IAI-4 films, which both possess the ENZ wavelength closer to 1.064 µm that is four times larger than that of pure ITO film, along with the β. Such enhancement is mainly ascribed to the ENZ effect. The refractive index change Δn follows the relation $\Delta n = \Delta\varepsilon/2\sqrt{\varepsilon}$[3], where $\Delta\varepsilon$ and ε are the change of dielectric permittivity and permittivity of materials, respectively. The Δn achieves its maximum value at the zero-permittivity wavelength. In the multilayer films, the complex nonlinear response $\tilde{n}_2$ of the composite films is written as $\tilde{n}_2 = 3\chi_{\text{eff}}^{(3)}/4\varepsilon_0 c n_0 \operatorname{Re}[n_0]$, where ε_0 is the vacuum permittivity, c is the speed of light in the vacuum, and n_0 is the refractive index of composite film. The reduced n_0 near the ENZ wavelength will increase the $\tilde{n}_2$, as reported in Ref. [8].

To further explore the causes of the optical nonlinearity enhancement, the carrier concentrations and resistivity measured by the four-probe Hall method are given, as shown in Table 1 and Fig. 5. The pure ITO film has the highest resistivity ($8.8 \times 10^{-4}\ \Omega \cdot$cm) and the lowest carrier concentration (1.3×10^{20} cm^{-3}). The values are effectively modified in the multilayer films with the introduction of Au layers. As the Au
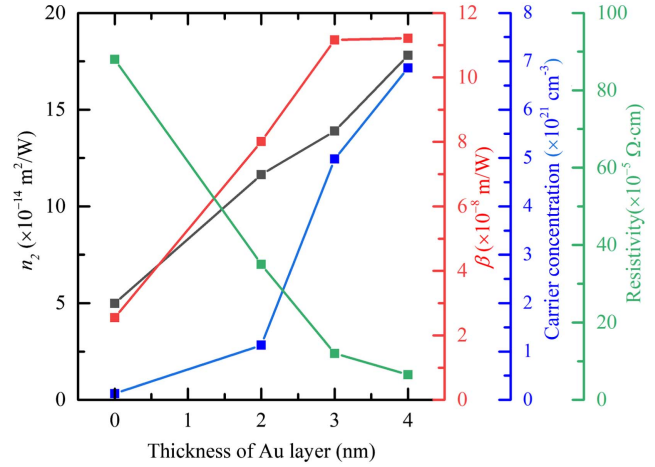
layer increases from 2 to 4 nm, the resistivity monotonically drops to $6.5 \times 10^{-5}\ \Omega \cdot$cm, and the carrier concentration rises to 6.9×10^{21} cm^{-3}. Note that the values of resistivity and carrier concentration are quite close to those reported in Ref. [5]. The n_2 and β synchronously change with carrier concentration, which indicate that besides the modulation of the ENZ wavelength the ITO/Au multilayer films also tune the carrier concentration to influence the optical nonlinearity and agree with the conclusions in Refs. [5,14]. The change of concentration in the multilayer films with the different thickness of the Au layer may be ascribed to the electron transport property and interface effect between the ITO and Au layers, as discussed in Ref. [5]. With the increase of the Au layer, the carrier mobility of the composite films will increase due to the low resistivity of thick bulk metal.

We noticed that there exists the large enhancement of the local field between the Ag islands to enhance the optical nonlinearity in ITO/Ag/ITO films[5]. We conducted the numerical simulation to obtain the local field distribution for our samples. However, no enhancement was found, even in the sample of the 4 nm Au layer. The reason may be that the Au particle is too small at the nonresonant wavelength of 1.064 µm.

4. Conclusions

In summary, we modulated the ENZ wavelength in the ITO/Au multilayer films by changing the thickness of the Au layer and confirmed the enhanced third-order nonlinearity in ITO/Au multilayer film at around the ENZ wavelength. The combination of noble metal and dielectric film possessing the ENZ wavelength at the infrared wavelength theoretically can tune the effective ENZ wavelength covering the UV to infrared regions, though the imaginary part of effective permittivity in multilayers should be balanced for optimized designs. The enhanced optical nonlinearity at the designed ENZ wavelength indicates that such

multilayer stacks offer a flexible platform for advanced all-optical devices.

Acknowledgement

References

1. R. W. Boyd, *Nonlinear Optics* (Academic Press, 2003).
2. O. Reshef, I. De Leon, M. Z. Alam, and R. W. Boyd, "Nonlinear optical effects in epsilon-near-zero media," Nat. Rev. Mater. **4**, 535 (2019).
3. M. Z. Alam, I. De Leon, and R. W. Boyd, "Large optical nonlinearity of indium tin oxide in its epsilon-near-zero region," Science **352**, 795 (2016).
4. M. Z. Alam, S. A. Schulz, J. Upham, I. De Leon, and R. W. Boyd, "Large optical nonlinearity of nanoantennas coupled to an epsilon-near-zero material," Nat. Photonics **12**, 79 (2018).
5. K. Wu, Z. W. Wang, J. H. Yang, and H. Ye, "Large optical nonlinearity of ITO/Ag/ITO sandwiches based on Z-scan measurement," Opt. Lett. **44**, 2490 (2019).
6. I. Liberal and N. Engheta, "Near-zero refractive index photonics," Nat. Photonics **11**, 149 (2017).
7. A. Capretti, Y. Wang, N. Engheta, and L. Dal Negro, "Comparative study of second-harmonic generation from epsilon-near-zero indium tin oxide and titanium nitride nanolayers excited in the near-infrared spectral range," ACS Photonics **2**, 1584 (2015).
8. S. Suresh, O. Reshef, M. Z. Alam, J. Upham, M. Karimi, and R. W. Boyd, "Enhanced nonlinear optical responses of layered epsilon-near-zero meta-materials at visible frequencies," ACS Photonics **8**, 125 (2021).
9. R. W. Boyd and J. E. Sipe, "Nonlinear optical susceptibility of layered composite materials," J. Opt. Soc. Am. B **11**, 297 (1994).
10. P. B. Johnson and R. W. Christy, "Optical constants of the noble metals," Phys. Rev. B **6**, 4370 (1972).
11. M. Sheik-Bahae, A. A. Said, T. H. Wei, D. J. Hagan, and E. W. Van Stryland, "Sensitive measurement of optical nonlinearities using a single beam," IEEE J. Quantum Electron. **26**, 760 (1990).
12. T. Ning, H. Lu, Y. Zhou, and B. Man, "Decrease and enhancement of third-order optical nonlinearity in metal-dielectric composite films," Appl. Phys. Lett. **112**, 151904 (2018).
13. T. Ning and Y. Zhou, "Effect of structure on nonlinear optical properties in $CaCu_3Ti_4O_{12}$ films," J. Appl. Phys. **118**, 233103 (2015).
14. H. I. Elim, W. Ji, and F. Zhu, "Carrier concentration dependence of optical Kerr nonlinearity in indium tin oxide films," Appl. Phys. B **82**, 439 (2006).